Coherent Vortices and Subharmonic Interactions in the Two-Dimensional Navier-Stokes Equations

H. T. Moon[a]

Department of Astrophysical, Planetary, and Atmospheric Sciences, University of Colorado, Boulder, Colorado 80309

(Received 12 May 1986)

2D Navier-Stokes solutions are generated for a periodic shear layer with a fundamental ($m=0$) and a single subharmonic ($m>0$) disturbance. For $m=2$, 3, and 4 we find clusters with $m+1$ vortices without the formation of vortex pairs. This implies enhanced spreading in a spatially growing mixing layer. However, when $m=5$ we find a different dynamical clustering due to nondirect energy transfer from the fundamental to the subharmonic. Additionally, if we force the layer with a wavelength smaller than the fundamental we find a new mechanism called "collective interaction."

PACS numbers: 47.90.+a, 47.20.−k, 47.25.Gk

In this Letter I present a numerical study of the subharmonic interactions displayed by coherent vortical structures in a two-dimensional shear layer governed by the Navier-Stokes equations. I believe that this work is related to current studies of turbulence, such as strong coupling between initial instability and subsequent flow development,[1,2] as well as to the relationship between highly coherent nonlinear excitations and states which exhibit deterministic turbulence.[3,4]

The basic shear flow to be studied is a parallel flow which has a broken-line velocity profile as shown in Fig. 1(a). The shear region, when undisturbed, is along the x axis. Linear theory[5] reveals that this flow is unstable to a sinusoidal disturbance of small amplitude. Figure 1(b) gives the linear growth rate as a function of wave number. The fastest-growing mode is called the fundamental and is found to be $k_0=0.4/d$, where d is one half of the shear thickness. The initial flow is in the form of the basic flow plus a small-amplitude sinusoidal perturbation. I represent the middle line of the shear layer (i.e., the x axis when undisturbed) by evenly distributing dyed fluid particles along the line. The distribution of dyed particles for the initially perturbed shear flow that we consider is expressed as

$$S(x,y,t=0)=\int\sum_{n=1}^{N_p}\delta(x-x_n)\delta[y-A_0\sin(k_0x_n)-A_m\sin(k_mx_n+\phi_m)]\,dx\,dy, \tag{1a}$$

$$k_m=k_0/(1+m), \quad m=1,2,3,4,\ldots, \tag{1b}$$

where k_m represents the mth subharmonic[6] of the fundamental k_0, A_m and A_0 are their small amplitudes, and ϕ_m and N_p denote a phase difference and a total number of particles, respectively. The evolution of the perturbed shear flow is determined by the time-dependent incompressible 2D Navier-Stokes equations, which are written as

$$d\omega/dt+\partial(\omega,\psi)/\partial(x,y)=\nu\nabla^2\omega, \tag{2a}$$

$$\nabla^2\psi=-\omega, \tag{2b}$$

where ω is the vorticity, ψ is the stream function, and ν is the kinematic viscosity. The streamwise and cross-stream velocities are given by $u=\partial\psi/\partial y$, $v=-\partial\psi/\partial x$, respectively. We look for numerical solutions to Eqs. (2) using a pseudospectral approximation[7] based on a $N_x\times N_y$ Fourier-series representation of the flow field in the spatial domain, $0\le x\le(1+m)\lambda_0$, and $-1.36\lambda_0\le y\le 1.36\lambda_0$. N_x is varied from 64 to 128 depending on the situation, and N_y is fixed at 64. The time differencing has been han-

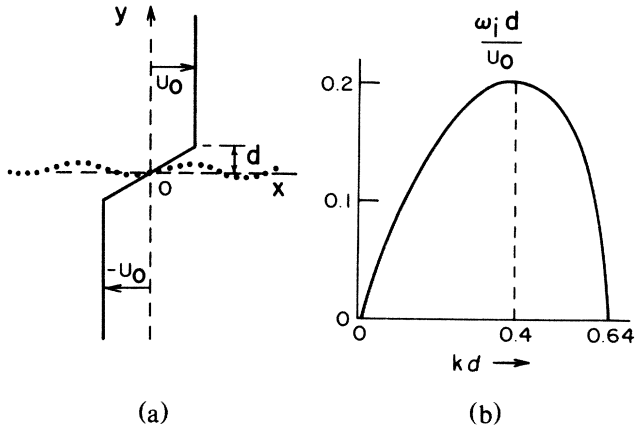

FIG. 1. (a) Basic shear flow and sketch of the test particles along the shear region. (b) Linear growth rate ω_i vs k, $k_0=0.4/d$.

dled by the leapfrog scheme as a predictor step followed by a trapezoidal corrector step.[8] The flow is periodic in x, and we require that the stream function $\psi(x,y,t)$ satisfy $\psi = U_0 y + \text{const}$ at $y = 1.36\lambda_0$ and $\psi = -U_0 y + \text{const}$ at $y = -1.36\lambda_0$, as well as $\partial^2\psi/\partial x^2 = 0$ at $y = +1.36\lambda_0$. I have chosen $\lambda_0 = 2.36$ cm, $U_0 = 2.52$ cm/sec, $d = 0.15$ cm, and the kinematic viscosity $\nu = 0.01$ cm^2/sec. The initial Reynolds number, based on these, becomes $N_{\text{Re}} = U_0 d/\nu = 37.80$, which corresponds to the experimental value.[1] The velocity of a dyed particle within a unit cell is calculated by area-weighted linear interpolation[9] from the values at the neighboring grid points. A total of as many as 3840 particles is used to show their positions and it is emphasized that they do not enter into the calculation at all.[9] The phase difference ϕ_m is set equal to 0, which value endows the dynamical system with special symmetry properties. The initial velocity distribution becomes, as a consequence of Eq. (1), odd under the operations $x \rightarrow -x$, $y \rightarrow -y$; i.e., $u(x,y) = -u(-x,-y)$, $v(x,y) = -v(-x,-y)$. This symmetry also implies that $\psi(x,y) = \psi(-x,-y)$ and $\omega(x,y) = \omega(x,y)$. This property is preserved in time because of the invariance of Eqs. (2) under the same operations. The symmetry property is constantly checked for the integrity of the current numerical simulations.

We first discuss the case when the basic flow is perturbed only by the fundamental. The subharmonic amplitude a_m in Eq. (1) is set equal to zero and the amplitude of the fundamental A_0 is given the value 0.06, which corresponds to an energy content of 1.0% of the mean flow energy. Figure 2 gives the evolution of the perturbed shear layer. The streak lines of Fig. 2(a) show the beginning of a rollup state at $t = 1.04\lambda_0/U_0$. Figure 2(b) gives the corresponding stream function, illustrating that the streak-line lumps are confined in regions enclosed by the closed contour lines of the stream function known as Kelvin's cat's eyes. The dyed fluid is seen to be trapped in the eyes and rolls around them constantly creating new interfaces. Figure 2(c) displays the sharp spiral structures developed later at $t = 3.3\lambda_0/U_0$. This observation is consistent with the theoretical prediction of Jimenez.[10] The creation of the sharp structures, however, needs the following explanation. The viscous dissipation is higher at the rollup state than at any other time because of the nonlinear excitation of higher harmonics of the fundamental. Because of the dissipation, the orbit of a fluid particle around an eye is not closed but rather is a shrinking spiral. The rollup state then relaxes while the system is subject to a viscous dissipation and is followed by a state of smaller discrete lumps but with finer spiral patterns in them, as shown in Fig. 2(c).

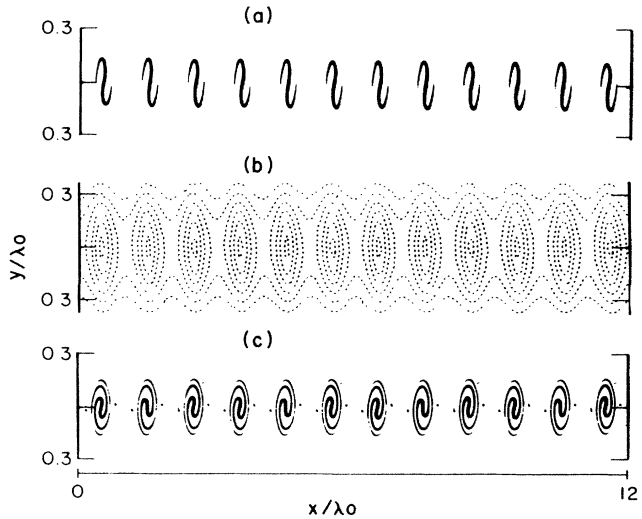

FIG. 2. (a) Streak lines at the rollup state, $t = 1.04\lambda_0/U_0$. (b) Corresponding stream function. (c) Streak lines at $t = 3.3\lambda_0/U_0$.

With a substantial amount of energy dissipated away, the system moves to a lower-energy state by activating a longer-wavelength mode. A great deal of experimental work has been devoted to the control of energy transfer to a particular mode, which changes the interaction pattern of discrete vortices downstream and therefore changes the growth of the layer. Recent experimental investigations[1,2] indicate that interactions between discrete vortices are not necessarily limited to pairings, but also involve three or more vortices. To investigate this within the deterministic models, the amplitude of the subharmonic A_m is now assigned a value 0.026 (0.5% of the mean flow energy) and $A_0 = 0.06$. When m is 1, i.e., when the system is further perturbed by the first subharmonic, a pairing of two neighboring vortices results at around $t \cong 1.0\lambda_m/U_0$, which case has been extensively studied.[11] When m is raised to 2 or 3, a vortex tripling or quadrupling is realized again at around $t \cong 1.0\lambda_m/U_0$ as shown in Figs. 3(a) and 3(b). A qualitatively similar behavior has been observed for $m = 4$ also, and Fig. 3(c) shows a cluster of five vortices at $t = 1.26\lambda_4/U_0$. To study the energetics of the simultaneous merging of multiple vortices, the cross-streamwise averaged, one-dimensional energy-dissipation spectrum[12] $D(k)$ is calculated. Figure 3(d) gives $D(k)$ for $m = 4$ at three different instants which are $t_0 = 1.2\lambda_0/U_0$, $t_1 = 3.8\lambda_0/U_0$, and $t_2 = 6.3\lambda_0/U_0$. It is noted that the rollup state of discrete vortices similar to the one shown in Fig. 2(a) is formed at $t_0 = 1.2\lambda_0/U_0$. As explained earlier, the rollup state is experiencing a high viscous dissipation for a while. Then, at $t_1 = 3.8\lambda_0/U_0$, it is observed that the line horizontally joining the vortices is only slightly tilted vertically, indicating the initial growth of the subharmonic (not shown here).

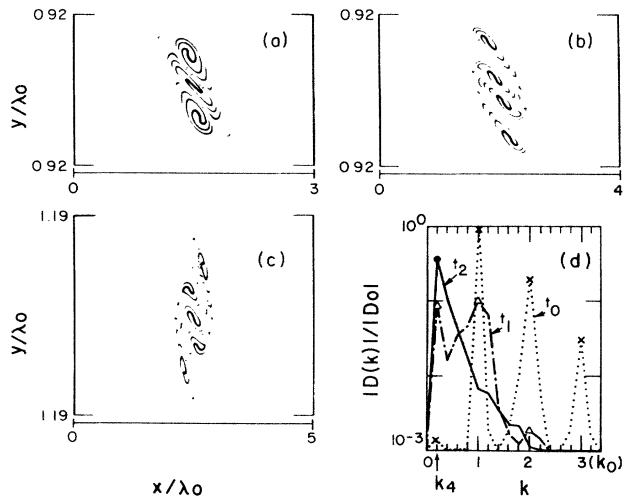

FIG. 3. Vortex clustering: (a) $m=2$, $t=3.7\lambda_0/U_0$; (b) $m=3$, $t=5.22\lambda_0/U_0$; (c) $m=4$, $t=6.3\lambda_0/U_0$, (d) Dissipation spectra $D(k)$ for $m=4$ at $t_0=1.2$, $t_1=3.8$, $t_2=6.3\lambda_0/U_0$. D_0 denotes $D(k_0,t_0)$.

Even at this instant, the dissipation spectrum of Fig. 3(d) points out that the fourth subharmonic is about to be the dominant mode. Figure 3(d) further indicates that this subharmonic is yet to grow, as the energy of the fundamental is selectively transferred to the fourth subharmonic, bypassing the instability modes in between. The selective growth of the fourth subharmonic results in the *simultaneous* merging of five vortices in the real space. The five vortices are almost vertically aligned [Fig. 3(c)] when the subharmonic reaches its peak at $t_2=6.3\lambda_0/U_0$, which is nearly five times the rollup time of $t_0=1.2\lambda_0/U_0$.

As the subharmonic is separated farther apart from the fundamental by the raising of m, the intermediate instability modes lying between the fundamental and the forced subharmonic are observed to become important. The dissipation spectrum of Fig. 4(a) shows that the forced subharmonic is overpowered by the intermediate modes in the course of the evolution at $t_1=5.2\lambda_0/U_0$ and $t_2=6.74\lambda_0/U_0$. Figure 4(b) gives the interaction of vortices at the corresponding moments in real space. Instead of the simultaneous merging of six vortices, a local pairing of two vortices is first seen at t_1. Later, at t_2, the unpaired vortex rolls around the paired one to merge. This in a sense resembles an unforced shear layer.[1] A_5 in Eq. (1a) has been raised from 0.026 to 0.6, but the resulting situation is still observed to be the same. A qualitatively similar behavior is observed for m greater than 5 if the natural vortices generated from the fundamental are involved. The participation of many instability modes in the dynamics now certainly creates more complicated flow motions.

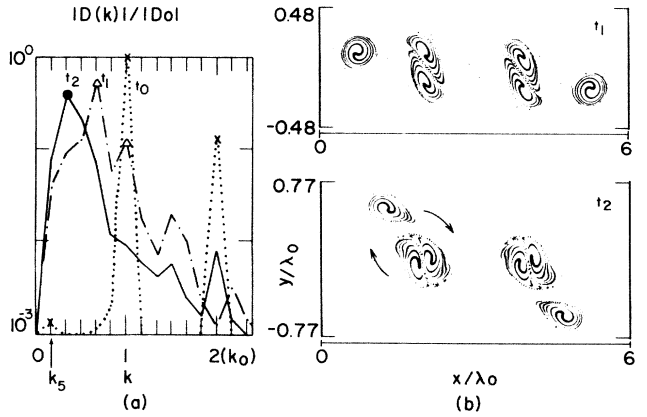

FIG. 4. (a) $D(k)$ for $m=5$ at $t_0=1.05\lambda_0/U_0$, $t_1=5.2\lambda_0/U_0$, and $t_2=6.74\lambda_0/U_0$. (b) Corresponding vortex interactions in real space.

A different dynamical clustering does take place when the vortices involved are physically smaller than the natural vortices. Figure 5 illustrates how this type of clustering occurs. The distance between the vortices shown in Fig. 5(a) is $\lambda_f=0.71\lambda_0$. These smaller vortices are generated from the instability mode of $k_f=1.4k_0$. When this state is further forced by *its* fifth subharmonic, i.e., by the mode of $k_f/6$, six such vortices coalesce at once, as shown in Figs. 5(b) and 5(c). Note that the streamwise spatial domain of Fig. 5 corresponds to the wave number $\Delta k=k_f/12$, which is big enough to have two large merged structures. The main feature of this interaction lies in the two characteristically different regions; one is a vortex-

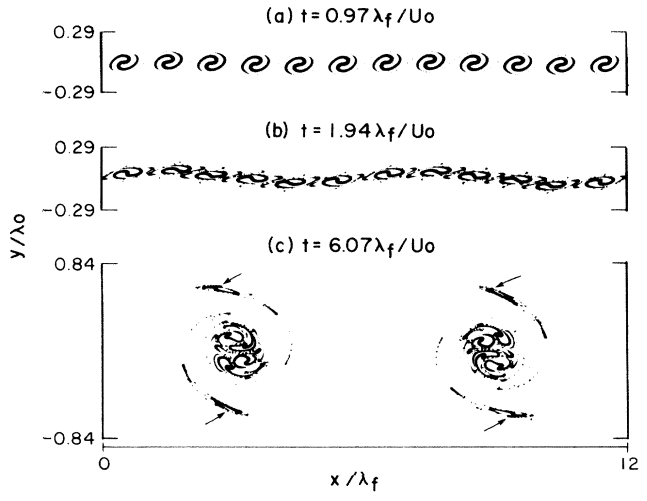

FIG. 5. A new mechanism, "collective interaction," $\lambda_f=\lambda_0/1.4$. Each cluster shows a collective interaction of six small vortices. The arrows indicate the far-stretched (migrating) vortices in each cluster, where two such vortices are enclosing the others merging at the center.

merging region at the center of the cluster and the other is a region where two individual vortices are far stretched, enclosing the central merging region. These stretched vortices are indicated by arrows in Fig. 5(c), and they separate clusters from each other. A larger number of vortices, from seven to ten, for example, are also tested, and it is found that they too can be made to interact all together to form a cluster like the one shown Fig. 5(c), as long as the vortices involved are made physically smaller. In all these cases, only two vortices are extremely stretched to encircle the central area where the merging of the rest of the vortices takes place. This kind of vortex merging was also observed in the laboratory experiments[1,2] and was referred to as a "collective interaction."[1] Investigation of the dissipation spectrum suggests that the smallness of the vortices involved makes the energy transfer easier from the forced mode to its particular subharmonic.

In summary, it is shown that the selective growth of a subharmonic involves a corresponding simultaneous merging of multiple vortices in real space. A control of this merging pattern bears on a significant practical implication because of the associated dramatic increase of the spreading rate. The direct energy transfer from the fundamental to a particular subharmonic is shown to be possible with the weak forcing of the subharmonic, as long as the subharmonic is not too far apart from the fundamental. When far apart, which may presumably depend on the initial noise level, the intermediate instability modes may grow faster, resulting in a local merging of small number of vortices which rather resembles an unforced shear layer. Since the interaction of vortices is largely determined by the long-wavelength subharmonic instability, the motion is basically inviscid. A collective interaction found in the laboratory is also shown to be a property of the two-dimensional Navier-Stokes equations. As a prerequisite for this new interaction, the vortices need to be smaller than the natural vortices. The actual physical size of the vortex may also seem to depend on the number of vortices involved in the interaction.

The author wishes to thank Dr. C.-M. Ho, Dr. P. Huerre, Dr. E. A. Novikov, and Dr. J. Toomre for many helpful discussions. He thanks the National Center for Atmospheric Research, supported by the National Science Foundation, for computer time used in this study. This work was supported by the National Science Foundation, Atmospheric Science Section (Grant No. ATM-8511906).

---

[a]Current address: Physics Department, Korea Institute of Technology, Daedukdanchi, Chung-Nam, Korea.

[1]C.-M. Ho and L. S. Huang, J. Fluid Mech. **119**, 443 (1982).

[2]I. Wygnansky, D. Oster, and F. Fiedler, in *Turbulent Shear Flows 2,* edited by L. J. S. Bradbury *et al.* (Springer-Verlag, New York, 1980).

[3]J. Laufer, in *Transition and Turbulence,* edited by R. E. Meyer (Academic, New York, 1981), p. 63.

[4]H. T. Moon and M. V. Goldman, Phys. Rev. Lett. **53**, 1821 (1984).

[5]P. G. Drazin and L. N. Howard, *Advances in Applied Mechanics* (Academic, New York, 1966), Vol. 9, p. 1.

[6]P. G. Saffman and R. Szeto, Stud. Appl. Math. **65**, 223 (1981).

[7]J. J. Riley and R. W. Metcalfe, AIAA Paper No. 80-0274, 1980.

[8]Jenö Gazdag, J. Comput. Phys. **20**, 196 (1976).

[9]Anthony A. Amsden and Francis H. Harlow, Phys. Fluids **7**, 327 (1964).

[10]J. Jimenez, J. Fluid Mech. **96**, 447 (1980).

[11]G. M. Corcos and F. S. Sherman, J. Fluid Mech. **139**, 29 (1984).

[12]N. J. Zabusky and G. S. Deem, J. Fluid Mech. **47**, 353 (1971).